ACS Macro Letters

Letter

pubs.acs.org/macroletters

In Situ Formation of Polymer–Gold Composite Nanoparticles with Tunable Morphologies

Richard Bleach,[†,#] Bunyamin Karagoz,[†,‡,§,#] Shyam M. Prakash,[‡] Thomas P. Davis,*[,∥,⊥] and Cyrille Boyer*[,†,‡]

[†]Centre for Advanced Macromolecular Design (CAMD), School of Chemical Engineering, University of New South Wales, Sydney NSW 2052, Australia

[‡]Australian Centre for Nanomedicine, The University of New South Wales, Sydney NSW 2052, Australia

[§]Istanbul Technical University Department of Chemistry, Maslak 34469 Istanbul, Turkey

[∥]ARC Centre of Excellence in Convergent Bio-Nano Science and Technology, Monash Institute of Pharmaceutical Sciences, Monash University, Parkville, VIC 3052, Australia

[⊥]Department of Chemistry, University of Warwick, Coventry CV4 7AL, United Kingdom

S *Supporting Information*

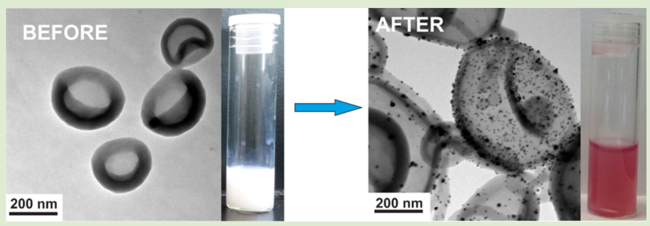

ABSTRACT: A simple and efficient route to gold–polymer nanoparticle composites is described. Our versatile synthetic route exerts facile control over polymer nanoparticle morphology, including micelles, rod-like structures, and vesicles, all easily attainable from a single polymerization taken to different monomer conversions. Specifically, poly[oligo(ethylene glycol) methacrylate]-*b*-poly(dimethylaminoethyl methacrylate)-*b*-poly(styrene) (POEGMA-*b*-PDMAEMA-*b*-PST) triblock copolymers were synthesized using a polymerization induced self-assembly (PISA) approach. Subsequently, spherical gold nanoparticles (10 nm AuNPs) were formed at the hydrophilic–hydrophobic nexus of the assembled triblock copolymer nanoaggregates by the addition of chloroauric acid ($HAuCl_4$) followed by in situ reduction using $NaBH_4$. After reduction, the cloudy white nanoparticle dispersions turned to a red-purple color. The gold nanoparticles that formed were stabilized by the enveloping polymeric nanostructures, neither precipitation nor agglomeration occurred. We demonstrated that we were able to tune the gold nanoparticle composition in these polymer–gold composites by varying the concentration of chloroauric acid. Morphology, particle size, molecular weight, AuNP content, and chemical structure of the polymer structures were characterized by transmittance electron microscopy (TEM), dynamic light scattering (DLS), size exclusion chromatography (SEC), thermal gravimetric analysis (TGA), and ^1H NMR. Finally, the formation of the AuNPs occurred without affecting the polymer nanoparticle morphology.

Polymer/inorganic hybrid nanoparticles have garnered much attention given their potential applications in a broad range of areas including biotechnology, nanotechnology, optoelectronics, therapeutic applications, and catalysis.[1] Specifically, gold nanoparticles (AuNPs) are widely studied as they are nontoxic, are tunable in size and shape, and a plasmon resonance band ranging from 500 to 800 nm.[2] However, AuNPs have a high surface area that results in poor colloidal stability and subsequent aggregation in solution.[3] To overcome this instability, polymers have often been used as an outer shell coating to the gold cores, providing a steric (or sometimes electrostatic) barrier to aggregation.[4] A slightly different approach to polymer–metal hybrid nanoparticles has also been taken, where inorganic nanoparticles (e.g., AuNPs, magnetic nanoparticles), have been attached to the surface of polymeric microparticles yielding composites with demonstrated potential in cancer therapy and photovoltaic applications.[5]

There have been a number of publications describing a combination of inorganic nanoparticles with polymeric particles, to produce colloidal composite particles with complex internal phases.[6] Most commonly, an ex situ approach is taken; a method based on the cooperative self-organization of preformed inorganic nanoparticles in the presence of presynthesized polymers as reported by Taton and co-workers, for instance, who encapsulated hydrophobic iron oxide nanoparticles into poly(acrylic acid)-*block*-poly(styrene) (PS-*b*-PAA) micelles.[7] In another example, Yabu and co-workers self-assembled inorganic nanoparticles in micelles, exploiting electrostatic interactions, generating a range of spherical composites.[8] In other work, So-Jung Park and co-workers self-assembled AuNPs in the hydrophobic layer of preformed PS-*b*-PAA or poly(ethylene oxide)-*block*-polylactide based vesicles.[9]

Received: April 2, 2014
Accepted: May 29, 2014
Published: June 10, 2014

Scheme 1. (A) Schematic illustration of POEGMA Homopolymer and POEGMA-*b*-PDMAEMA Diblock Copolymer Synthesis (Left) and Their SEC Traces (Right); (B) Schematic Illustration of Dispersion Polymerization of Styrene in the Presence of POEGMA-*b*-PDMAEMA (Top); SEC Traces of the POEGMA-*b*-PDMAEMA-*b*-PST Triblock Copolymers at Different Polymerization Times (Bottom-Left); Evolution of Molecular Weight and PDI versus Monomer Conversion (Bottom-Right)

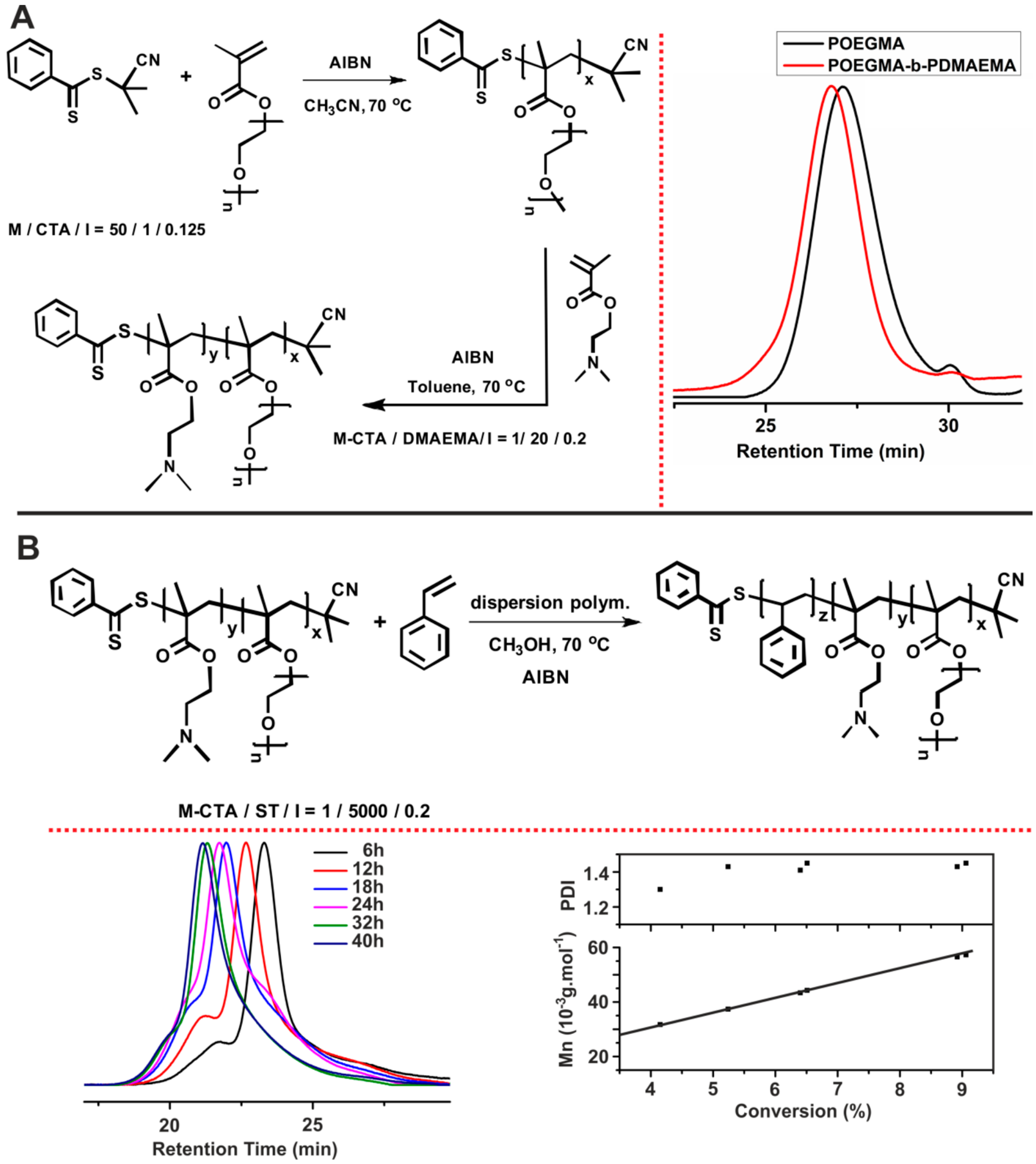

An alternative synthetic approach to prepare hybrid organic/inorganic nanocomposites is the in situ production of inorganic nanoparticles within preformed polymeric nanoparticles.[6a,10] In this method, one of the polymer blocks strongly interacts with the metallic (precursor) ion.[10b,11] Metal–polymer composite particles are subsequently generated via the direct reduction of the metallic precursors contained within polymeric nanoparticles. As an example, McCormick and co-workers synthesized gold nanoparticles inside spherical polymersomes using the in situ reduction of chloroauric acid in the presence of tertiary amine groups.[12]

To our best knowledge, no work has been done on the preparation of polymer-gold composite with diverse shapes, ranging from spherical and rod-like micelles to vesicles. In this paper, we present a simple and versatile method for the preparation of tunable hybrid nanocomposite morphologies composed of a polymer nanostructure, enveloping multiple spherical gold nanoparticles. We exploited polymerization-induced self-assembly (PISA)[13] together with in situ gold nanoparticle formation, in a novel synthetic strategy to generate these composite nanoparticles. We were able to tune the content of the spherical gold nanoparticles at the interface of hydrophilic and hydrophobic segments.

Polymerization-Induced Self-Assembled (PISA) Approach: OEGMA (M_n = 300 g mol^{-1}) was polymerized by reversible addition–fragmentation chain transfer (RAFT) polymerization,[14] yielding POEGMA ($M_{n,SEC}$ = 7300 g mol^{-1} and PDI = 1.08). The PEOGMA was then chain extended in the presence of dimethylaminoethyl methacrylate (DMAEMA) in toluene (Scheme 1), yielding a diblock polymer (constituted by 15 units of DMAEMA), as verified by SEC analysis. The diblock copolymer was then chain extended using RAFT dispersion polymerization of styrene at 70 °C in methanol, to yield a triblock copolymer, as confirmed by SEC (Scheme 1B). Linear

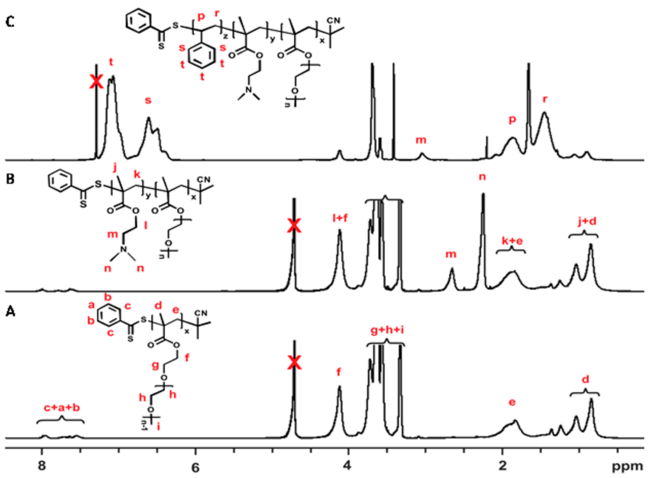

Figure 1. ^{1}H NMR spectra of (A) POEGMA recorded in D_2O, (B) POEGMA-*b*-PDMAEMA block copolymer recorded in D_2O, and (C) POEGMA-*b*-PDMAEMA-*b*-PST recorded in *d*-chloroform.

Table 1. Summary of the Polymers Prepared in This Study

#	α^a (%)	$M_{n,NMR}{}^b$ (g mol^{-1})	$M_{n,SEC}{}^c$ (g mol^{-1})	PDI^c
POEGMA	42	7700	7300	1.08
POEGMA-*b*-PDMAEMA	75	8800	8500	1.09
time (h)		POEGMA-*b*-PDMAEMA-*b*-PST		
6	4.2	31700	22000	1.30
12	5.3	37400	24400	1.43
18	6.3	43400	28900	1.45
24	6.5	44300	32100	1.41
32	8.9	56550	37000	1.43
40	9.1	57300	37600	1.45

^{a}Monomer conversion was calculated from ^{1}H NMR spectrum. ^{b}NMR molecular weight was calculated according to this equation $M_n = ([M]_0/[RAFT]_0) \times \alpha \times M_w^{monomer} + M_w^{RAFT}$, where $[M]_0$, $[RAFT]_0$, α, $M_w^{monomer}$, and M_w^{RAFT} are the monomer RAFT agent concentration and monomer conversion molecular weight of monomer and RAFT agent, respectively (Note: for POEGMA-*b*-PDMAEMA and POEGMA-*b*-PDMAEMA-*b*-PST copolymers, we used the molecular weight of POEGMA and POEGMA-*b*-PST as the molecular weight of the RAFT agent. ^{c}The experimental M_n and PDI were determined by SEC calibrated with polystyrene standards using *N,N*-dimethylacetamide as eluent.

increments in $\ln([M]_0/[M])$ and molecular weight with conversion, together with reasonably narrow PDIs demonstrate traits of livingness imbued by RAFT control over the dispersion polymerization (Scheme 1B). The molecular weight shoulders of POEGMA-*b*-PDMAEMA-*b*-PST triblock copolymers were observed at different polymerization times and were attributed to the formation of PST−PST radical coupling during the dispersion polymerization. Similar observations were also noted in previous publications using dispersion polymerization.[13d,15]

Styrene conversion increased continuously during the dispersion polymerization, attaining 9.1% after 40 h. The clear reaction solution became cloudy after 6 h of polymerization, finally turning milky-white at the end of the dispersion polymerization. SEC analysis confirmed the successful chain extension of POEGMA-*b*-PDMAEMA with a gradual increase of the molecular weight as the dispersion polymerization progressed (Scheme 1B).

The POEGMA homopolymer, POEGMA-*b*-PDMAEMA diblock copolymer, and POEGMA-*b*-PDMAEMA-*b*-PST triblock copolymers were all characterized by ^{1}H NMR (Figure 1). Characteristic signals of POEGMA homopolymer were observed between 4.3 and 3.3 ppm with dithiobenzoate end groups at 7.2, 7.5, and 7.8 ppm. After chain extension with PDMAEMA, new signals appeared at 2.55 and 2.30 ppm, consistent with methylene protons adjacent to the tertiary amino group and methyl protons on the tertiary amine besides POEGMA peaks in the midspectrum. After the final chain extension, the presence of aromatic protons of polystyrene at around 6.6 and 7.1 ppm confirmed triblock copolymer formation. ^{1}H NMR was also employed to estimate the molecular weight of the triblock copolymers (Table 1). The molecular weight values determined by SEC were slightly lower than the values calculated via NMR. Finally, FTIR spectroscopy (SI, Figure S1) was utilized to characterize the copolymers.

The morphologies that formed during the dispersion polymerization were investigated by TEM and DLS measurements. Number-average particle sizes of the triblock copolymers were measured as 34 nm after 6 h polymerization time and 436 nm after 40 h as depicted in Figure 2A. TEM images revealed morphology transitions with increasing monomer conversion, going from micelles to rod-like structures and then to vesicles (Figure 2B, and SI, Figure S2). The morphology progression was mainly influenced by the DP_n of the PST block, as shown in Figure 2C. Micelles were observed after the PST block reached 200 repeating units, and finally, vesicles were formed with 440 PST repeating units.

AuNP−Polymer Composite Formation: The triblock copolymer nanoaggregate dispersions were used for in situ gold nanoparticle formation exploiting the PDMAEMA block segment. Chloroauric acid was complexed with the tertiary amine groups present in DMAEMA using two different molar feed ratios, that is, 2:1 and 4:1 of Au/tertiary amine for 1 day. During the incubation, no self-reduction was observed. Reduction to form gold nanoparticles was achieved by adding a solution of $NaBH_4$ in water whereupon, the white cloudy dispersions turned to red-purple color in a few seconds (Figure 3A). The same protocol was followed for all the polymer morphologies (SI, Table S1).

Aliquots of the composite polymer-AuNPs were dried as thin films on a Mica substrate and the crystalline structures were investigated via XRD measurements (Figure 3C). In the XRD patterns, peaks at 38, 44, and 64° were observed, confirming the formation of metallic gold in a face-centered cubic lattice within the triblock copolymer aggregates. The peaks assigned using blue marks came from residual NaCl produced during the reduction. The presence of gold nanoparticles was also confirmed by TEM in Figure 3E (supplementary TEM micrographs are included in SI, see Figure S3), where gold nanoparticles can be seen as small black dots (≈10 nm). As clearly seen from the TEM images, the polymeric morphologies were not affected by the gold nanoparticle formation. According to the molar feed ratio of Au/tertiary amine, TEM revealed different densities of AuNPs encapsulated in the polymer composites, which demonstrated that the amount of AuNPs can be easily tuned using this approach (SI, Figure S4). As expected, greater density of AuNPs was observed when a high ratio of Au: tertiary amine was employed.

In addition, DLS also confirmed that the polymeric nanoparticle sizes were not affected by the gold attachment (Figure 3D). Furthermore, UV−visible spectroscopy showed

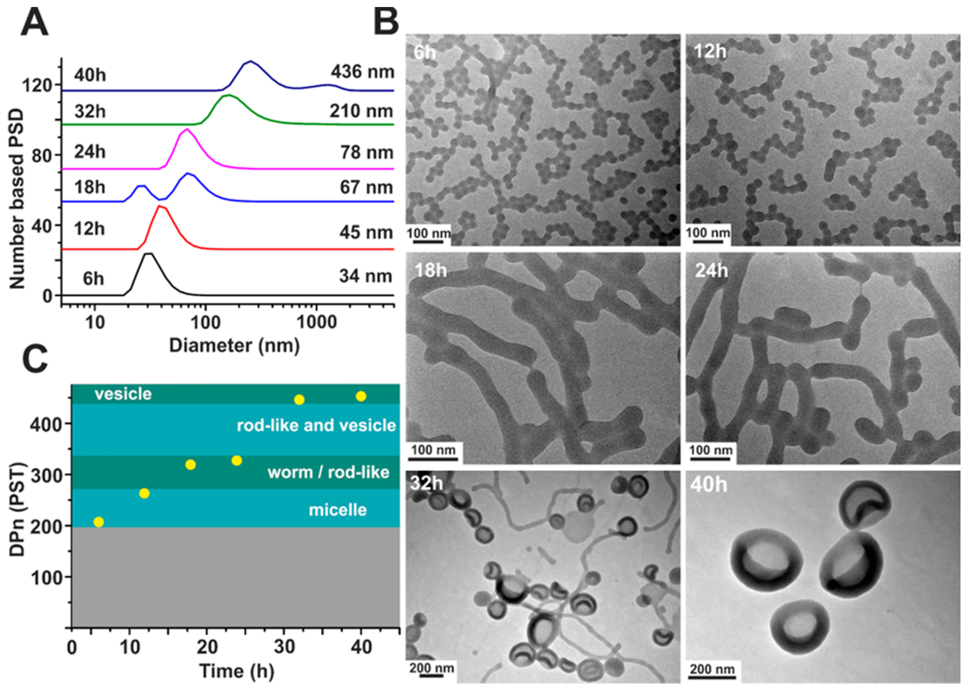

Figure 2. (A) Dynamic light scattering (DLS) of the solutions after dispersion polymerizations were taken to different polymerization times; (B) Transmission electron microscopy (TEM) of the different polymerization solutions after dialysis against methanol; (C) A phase diagram summary showing structural changes at different polymerization times.

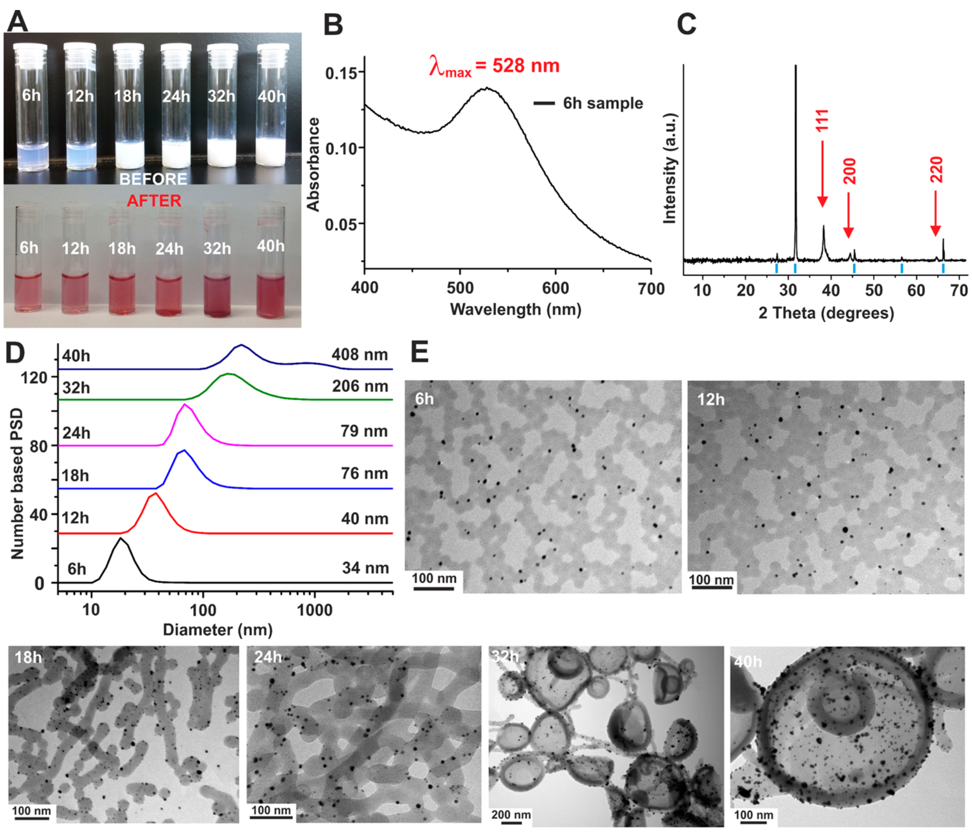

Figure 3. (A) Photographs of samples before and after reduction of chloroauric acid with $NaBH_4$; (B) A typical UV−visible spectrum of solution after reduction of chloroauric acid using $NaBH_4$; (C) XRD patterns of gold tethered POEGMA-*b*-PDMAEMA-*b*-PST nanoparticles (24 h sample); (D) Dynamic light scattering (DLS) of gold tethered POEGMA-*b*-PDMAEMA-*b*-PST nanoparticles; and (E) Transmission electron microscopy (TEM) micrographs of the gold decorated triblock copolymer nanoaggregates in aqueous dispersion obtained using a molar feed ratio, that is, 4:1 of Au/tertiary amine.

the presence of a visible absorption at 528 nm caused by the surface plasmon resonance (SPR effect) of AuNPs (Figure 3B),[16] which demonstrated the formation of spherical AuNP with a diameter of 10 nm. The characteristic wavelength of maximum absorption of plasmon resonance band and its width depends on the size, shape, and dielectric environment of the AuNPs.[17] Typically spherical AuNPs dispersed in water present a single absorption maximum which varies with their diameter.[18] The SPR wavelength exhibits a red-shift with any increase in nanoparticle size, along with an overall decrease in the maximum absorbance intensity. A stable, well dispersed solution of AuNPs appears red, as the average interparticle distance is greater than the particle diameter. When particle aggregation occurs, with the average interparticle distance becoming smaller than the particle diameter, the solution turns blue.[17] Finally, the SPR effect is also a function of the effective refractive index of the metal surface that is determined by the mass of the substances present at the interface.[18a]

TGA analysis was invoked after purification to determine the gold composition in the host POEGMA-*b*-PDMAEMA-*b*-PST triblock copolymer matrices. The amount of AuNPs present in the nanocomposites assessed by TGA varied from 8 to 20%, according to the molar feed ratio of Au/tertiary amine employed 2:1 and 4:1, respectively (SI, Table S1 and Figure S5).

In summary, we used polymerization induced self-assembly (PISA) to prepare different polymeric nanoparticle morphologies containing a short block of tertiary amine groups (DP_n = 15 units). The amino groups were exploited to complex gold ions, which were subsequently reduced by exposure to sodium borohydride ($NaBH_4$), yielding gold nanoparticles within the polymeric particles. These composites are currently investigated for catalysis and for bioapplications.

■ ASSOCIATED CONTENT

Supporting Information

Experimental section, Table S1, and Figures S1−S3. This material is available free of charge via the Internet at http://pubs.acs.org.

■ AUTHOR INFORMATION

Corresponding Authors

*E-mail: thomas.p.davis@monash.edu.

*E-mail: cboyer@unsw.edu.au.

Author Contributions

#These authors contributed equally.

Notes

The authors declare no competing financial interest.

■ ACKNOWLEDGMENTS

B.K. is thankful to the Scientific and Technological Research Council of Turkey (TUBITAK) for financial support. C.B. is thankful for his APD and Future Fellowship from Australian Research Council (ARC).

■ REFERENCES

(1) (a) Hirsch, L. R.; Stafford, R. J.; Bankson, J. A.; Sershen, S. R.; Rivera, B.; Price, R. E.; Hazle, J. D.; Halas, N. J.; West, J. L. *Proc. Natl. Acad. Sci. U.S.A.* **2003**, *100*, 13549−13554. (b) Kityk, I. V.; Ebothé, J.; Fuks-Janczarek, I.; Umar, A. A.; Kobayashi, K.; Oyama, M.; Sahraoui, B. *Nanotechnology* **2005**, *16*, 1687. (c) Han, M.; Gao, X.; Su, J. Z.; Nie, S. *Nat. Biotechnol.* **2001**, *19*, 631−635. (d) Boyer, C.; Whittaker, M. R.; Bulmus, V.; Liu, J.; Davis, T. P. *NPG Asia Mater.* **2010**, *2*, 23−30.

(2) (a) Kelly, K. L.; Coronado, E.; Zhao, L. L.; Schatz, G. C. *J. Phys. Chem. B* **2002**, *107*, 668−677. (b) Chen, J.; Saeki, F.; Wiley, B. J.; Cang, H.; Cobb, M. J.; Li, Z.-Y.; Au, L.; Zhang, H.; Kimmey, M. B.; Li; Xia, Y. *Nano Lett.* **2005**, *5*, 473−477. (c) Skrabalak, S. E.; Chen, J.; Sun, Y.; Lu, X.; Au, L.; Cobley, C. M.; Xia, Y. *Acc. Chem. Res.* **2008**, *41*, 1587−1595. (d) Liu, X.; Huang, N.; Li, H.; Wang, H.; Jin, Q.; Ji, J. *ACS Appl. Mater. Interfaces* **2014**, *6*, 5657−5668.

(3) Zhou, J.; Ralston, J.; Sedev, R.; Beattie, D. A. *J. Colloid Interface Sci.* **2009**, *331*, 251−262.

(4) (a) Shan, J.; Tenhu, H. *Chem. Commun.* **2007**, 4580−4598. (b) Boyer, C.; Bulmus, V.; Priyanto, P.; Teoh, W. Y.; Amal, R.; Davis, T. P. *J. Mater. Chem.* **2009**, *19*, 111−123. (c) Boyer, C.; Whittaker, M. R.; Luzon, M.; Davis, T. P. *Macromolecules* **2009**, *42*, 6917−6926.

(5) (a) Du, H.; Cao, Y.; Bai, Y.; Zhang, P.; Qian, X.; Wang, D.; Li, T.; Tang, X. *J. Phys. Chem. B* **1998**, *102*, 2329−2332. (b) Kubo, S.; Diaz, A.; Tang, Y.; Mayer, T. S.; Khoo, I. C.; Mallouk, T. E. *Nano Lett.* **2007**, *7*, 3418−3423. (c) Lee, J.-H.; Kim, D. O.; Song, G.-S.; Lee, Y.; Jung, S.-B.; Nam, J.-D. *Macromol. Rapid Commun.* **2007**, *28*, 634−640. (d) Hirsch, L. R.; Jackson, J. B.; Lee, A.; Halas, N. J.; West, J. L. *Anal. Chem.* **2003**, *75*, 2377−2381. (e) Liang, Z.; Susha, A. S.; Caruso, F. *Adv. Mater.* **2002**, *14*, 1160−1164.

(6) (a) Kim, M. P.; Kang, D. J.; Jung, D.-W.; Kannan, A. G.; Kim, K.-H.; Ku, K. H.; Jang, S. G.; Chae, W.-S.; Yi, G.-R.; Kim, B. J. *ACS Nano* **2012**, *6*, 2750−2757. (b) Bockstaller, M. R.; Lapetnikov, Y.; Margel, S.; Thomas, E. L. *J. Am. Chem. Soc.* **2003**, *125*, 5276−5277. (c) Chiu, J. J.; Kim, B. J.; Kramer, E. J.; Pine, D. J. *J. Am. Chem. Soc.* **2005**, *127*, 5036−5037. (d) Lopes, W. A.; Jaeger, H. M. *Nature* **2001**, *414*, 735−738. (e) Lim, J.; Yang, H.; Paek, K.; Cho, C.-H.; Kim, S.; Bang, J.; Kim, B. J. *J. Polym. Sci., Part A: Polym. Chem.* **2011**, *49*, 3464−3474. (f) Jang, S. G.; Khan, A.; Dimitriou, M. D.; Kim, B. J.; Lynd, N. A.; Kramer, E. J.; Hawker, C. J. *Soft Matter* **2011**, *7*, 6255−6263. (g) Mai, Y.; Eisenberg, A. *Acc. Chem. Res.* **2012**, *45*, 1657−1666. (h) Hickey, R. J.; Haynes, A. S.; Kikkawa, J. M.; Park, S.-J. *J. Am. Chem. Soc.* **2011**, *133*, 1517−1525.

(7) Kim, B.-S.; Qiu, J.-M.; Wang, J.-P.; Taton, T. A. *Nano Lett.* **2005**, *5*, 1987−1991.

(8) Kanahara, M.; Shimomura, M.; Yabu, H. *Soft Matter* **2014**, *10*, 275−280.

(9) Hickey, R. J.; Luo, Q.; Park, S.-J. *ACS Macro Lett.* **2013**, *2*, 805−808.

(10) (a) Misner, M. J.; Skaff, H.; Emrick, T.; Russell, T. P. *Adv. Mater.* **2003**, *15*, 221−224. (b) Koh, H.-D.; Park, S.; Russell, T. P. *ACS Nano* **2010**, *4*, 1124−1130. (c) Sohn, B. H.; Seo, B. H. *Chem. Mater.* **2001**, *13*, 1752−1757.

(11) Nash, M. A.; Lai, J. J.; Hoffman, A. S.; Yager, P.; Stayton, P. S. *Nano Lett.* **2009**, *10*, 85−91.

(12) (a) Li, Y.; Smith, A. E.; Lokitz, B. S.; McCormick, C. L. *Macromolecules* **2007**, *40*, 8524−8526. (b) Smith, A. E.; Xu, X.; Abell, T. U.; Kirkland, S. E.; Hensarling, R. M.; McCormick, C. L. *Macromolecules* **2009**, *42*, 2958−2964.

(13) (a) Karagoz, B.; Boyer, C.; Davis, T. P. *Macromol. Rapid Commun.* **2013**, DOI: 10.1002/marc.201300730 (b) Karagoz, B.; Esser, L.; Duong, H. T.; Basuki, J. S.; Boyer, C.; Davis, T. P. *Polym. Chem.* **2014**, *5*, 350−355. (c) Blanazs, A.; Armes, S. P.; Ryan, A. J. *Macromol. Rapid Commun.* **2009**, *30*, 267−277. (d) Blanazs, A.; Ryan, A. J.; Armes, S. P. *Macromolecules* **2012**, *45*, 5099−5107. (e) Sun, J.-T.; Hong, C.-Y.; Pan, C.-Y. *Soft Matter* **2012**, *8*, 7753. (f) Sun, J.-T.; Hong, C.-Y.; Pan, C.-Y. *Polym. Chem.* **2013**, *4*, 873. (g) Wan, W. M.; Hong, C. Y.; Pan, C. Y. *Chem. Commun.* **2009**, 5883−5885.

(14) (a) Boyer, C.; Bulmus, V.; Davis, T. P.; Ladmiral, V.; Liu, J.; Perrier, S. *Chem. Rev.* **2009**, *109*, 5402−5436. (b) Boyer, C.; Stenzel, M. H.; Davis, T. P. *J. Polym. Sci., Part A: Polym. Chem.* **2011**, *49*, 551−595.

(15) (a) Blanazs, A.; Madsen, J.; Battaglia, G.; Ryan, A. J.; Armes, S. P. *J. Am. Chem. Soc.* **2011**, *133*, 16581−16587. (b) Rosselgong, J.; Blanazs, A.; Chambon, P.; Williams, M.; Semsarilar, M.; Madsen, J.; Battaglia, G.; Armes, S. P. *ACS Macro Lett.* **2012**, *1*, 1041−1045. (c) Chambon, P.; Blanazs, A.; Battaglia, G.; Armes, S. P. *Langmuir* **2011**, *28*, 1196−1205.

(16) Coffer, J. L.; Shapley, J. R.; Drickamer, H. G. *J. Am. Chem. Soc.* **1990**, *112*, 3736−3742.
(17) Elghanian, R.; Storhoff, J. J.; Mucic, R. C.; Letsinger, R. L.; Mirkin, C. A. *Science* **1997**, *277*, 1078−1081.
(18) (a) Sota, H.; Hasegawa, Y.; Iwakura, M. *Anal. Chem.* **1998**, *70*, 2019−2024. (b) Boyer, C.; Whittaker, M. R.; Chuah, K.; Liu, J.; Davis, T. P. *Langmuir* **2009**, *26*, 2721−2730.